The Galaxy Disk in Cosmological Context
Proceedings IAU Symposium No. 254, 2008
J. Andersen, J. Bland–Hawthorn & B. Nordström, eds.

doi:10.1017/S1743921308027725

H I in Galactic Disks

Elias Brinks[1], Frank Bigiel[2], Adam Leroy[2], Fabian Walter[2], W. J. G. de Blok[3], Ioannis Bagetakos[1], Antonio Usero[1], and Robert C. Kennicutt, Jr.[4]

[1]Centre for Astrophysics Research, University of Hertfordshire, Hatfield AL10 9AB, UK
[2]Max–Plank–Institut für Astronomie, Königstuhl 17, 69117, Heidelberg, Germany
[3]Univ. of Cape Town, Dept. of Astronomy, Private Bag X3, Rondebosch 7701, South Africa
[4]Institute of Astronomy, University of Cambridge, Madingley Road, Cambridge CB3 0HA, UK

Abstract. Studies of the atomic phase of the interstellar medium, via the 21–cm spectral line of neutral hydrogen (H I), play a key rôle in our attempts to understand the structure and evolution of disk galaxies. We present here results from The H I Nearby Galaxy Survey (THINGS) and focus on the mass distribution as derived from the observed kinematics, and on the link between gas and star formation rate surface density, i.e., the Schmidt–Kennicutt law. Also, we briefly dwell on the wealth and wide variety of structures, often outlining what seem to be expanding shells surrounding sites of recent, massive star formation.

Keywords. galaxies: structure, galaxies: spiral, galaxies: ISM

1. Introduction

Results coming from The H I Nearby Galaxy Survey (THINGS) are beginning to shed new light on the structure and properties of galaxy disks. The THINGS team have observed 34 galaxies with the NRAO† Very Large Array in its B–, C–, and D–configuration, resulting in maps at a spatial resolution of $6''$. The velocity resolution is $5.2\,\mathrm{km\,s^{-1}}$ or better and the observations reach typical 1σ column density sensitivities of $4\times10^{19}\ \mathrm{cm^{-2}}$ at $30''$ resolution. Full details regarding the observations and data reduction can be found in Walter *et al.* (2008). THINGS covers a wide range of Hubble types, star formation rates, absolute luminosities, and metallicities and is being used to address key science questions regarding the kinematics and matter distribution in galaxies (de Blok *et al.* 2008; Oh *et al.* 2008; Trachternach *et al.* 2008), their star formation properties (Bigiel *et al.* 2008; Leroy *et al.* 2008a) and the structure of the ISM (Bagetakos *et al.* 2008; Usero *et al.* 2008). Results from a study assessing the extent of the neutral gas disks and what causes them to drop sharply in surface brightness were presented at this meeting as a poster by Portas (this volume) whereas some of the results derived by Leroy *et al.* (2008a) were highlighted in the talk by Blitz (this volume).

Most of the galaxies in THINGS were drawn from the *Spitzer* Infrared Nearby Galaxies Survey (SINGS; Kennicutt *et al.* 2003), a multi-wavelength project designed to study the properties of the dusty ISM in nearby galaxies. This ensures that multi–wavelength observations for each galaxy are available for further analysis. To this aim we also collaborate with the team running the *GALEX* (Galaxy Evolution Explorer) Nearby Galaxies Survey (Gil de Paz *et al.* 2007). Our final resolution of $6''$ is well matched to that of the *Spitzer* Space Telescope (e.g., resolution at $24\,\mu$m: $6''$) and *GALEX* (resolution in the Near–Ultraviolet: $5''$). A further crucial ingredient in several of the papers which

† The National Radio Astronomy Observatory is a facility of the National Science Foundation operated under cooperative agreement by Associated Universities, Inc.

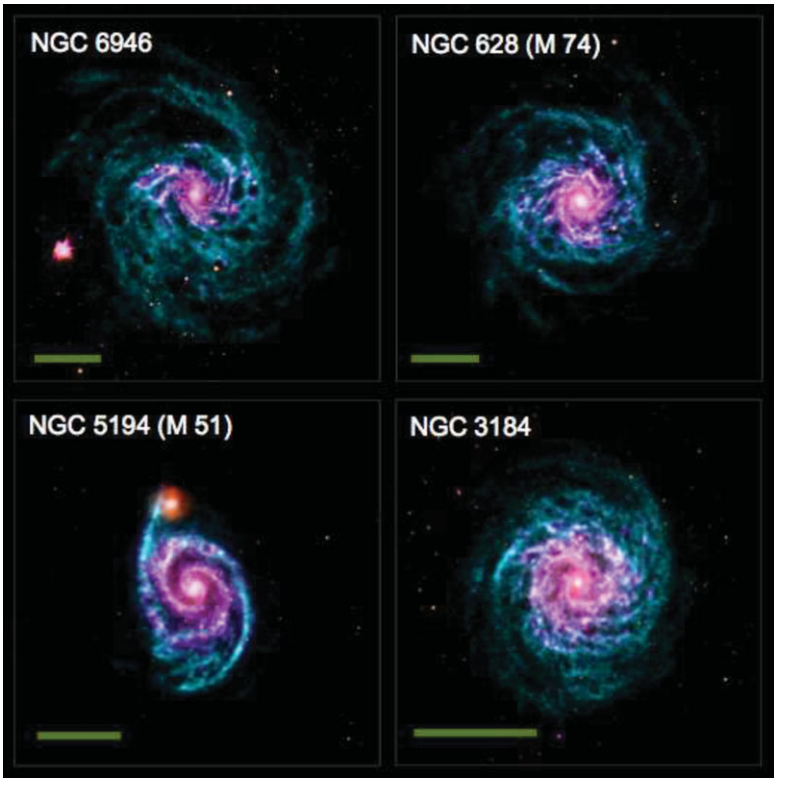

Figure 1. Some examples of spiral galaxies observed as part of THINGS. The H I emission is colour–coded in blue, the older stellar population is assigned an orange hue. Purple is a measure of the recent star formation activity and is a linear combination of the FUV flux measured with *GALEX*, and *Spitzer* 24 μm emission. The green bar measures 10 kpc.

are currently being prepared by us for publication is access to high quality CO observations. This is being provided by a parallel survey (HERACLES) with the HERA array of the IRAM 30–m telescope of 18 THINGS galaxies which we observed in the CO(2-1) transition (Leroy *et al.* 2008b).

Fig. 1 shows a mosaic of false colour composites for four spiral galaxies (see figure caption for details). The figure illustrates the quality achieved by THINGS and gives an indication of what can be achieved by combining THINGS with SINGS and *GALEX* data. In the sections which follow, we will highlight a few of the aspects of the analysis which is currently in progress.

2. Kinematics and Mass models

In the paper by de Blok *et al.* (2008) we present a rotation curve analyis of 19 galaxies. These are the highest quality H I rotation curves available to date for a large sample of nearby galaxies, spanning a wide range of H I masses and luminosities. The high quality of the data allows us to systematically derive the geometrical and dynamical parameters using H I data alone, for a much larger sample than has hitherto been possible. Fig. 2 illustrates how the analysis is performed.

We do not find any declining rotation curves unambiguously associated with a cut–off in the mass distribution out to the last measured point. The rotation curves are combined with 3.6 μm data from SINGS to construct mass models. Our best–fit dynamical disk

https://doi.org/10.1017/S1743921308027725 Published online by Cambridge University Press

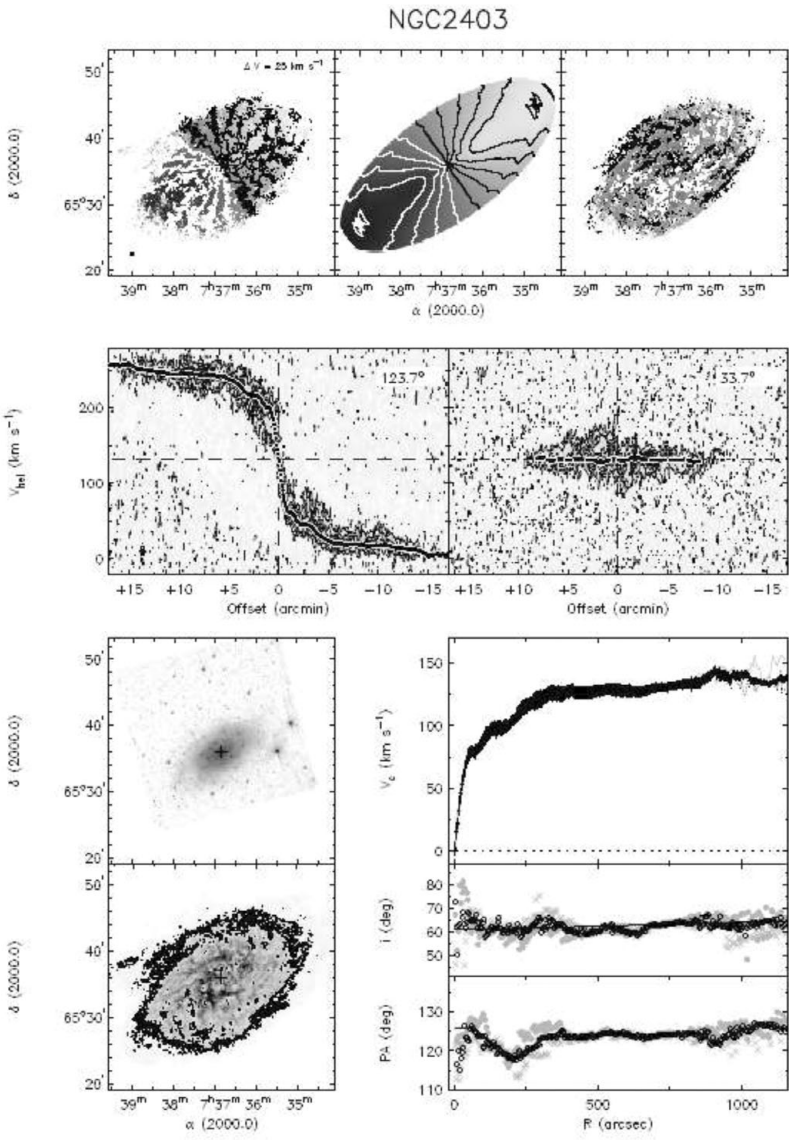

Figure 2. Tilted–ring analysis of the galaxy NGC 2403. The top row shows the observed velocity field (left), the tilted–ring model (centre), and residuals (right). The systemic velocity is indicated by the thick contour. The approaching side can be identified by the light gray–scales and the dark contours. The adopted dynamical center is indicated with a cross. The beam size is indicated by the ellipse in the bottom–left corner. The centre row presents a position–velocity cut along the major (left) and minor axis (right). The systemic velocity and position of the center are indicated by dashed lines. Over–plotted is the rotation curve projected onto the average major axis using the derived radial variations of PA and i. The bottom left panel shows at the top a *Spitzer* 3.6 μm emission map and at the bottom the H I surface brightness map. The bottom right panel is made up of the derived rotational velocity (top), inclination (middle) and position angle of the receding kinematical major axis (bottom) as a function of radius (figure taken from de Blok *et al.* 2008).

https://doi.org/10.1017/S1743921308027725 Published online by Cambridge University Press

masses, derived from the rotation curves, are in good agreement with photometric disk masses derived from the 3.6 μm images in combination with stellar population synthesis arguments. This implies that we can use the 3.6 μm maps to infer the stellar mass rather than having to assume a maximum disk for the stellar component, and thus removing considerable uncertainty in the determination of the mass profile of the non–baryonic matter. The stellar mass–modelling is described in detail in the papers by de Blok *et al.* (2008) and Leroy *et al.* (2008a). We also confirm that lower mass (dwarf) systems are dark matter dominated throughout: whereas in high mass galaxies the baryonic mass within the radius where the peak disk rotational velocity is found, can account for the velocity observed, in lower mass systems about 50% of the matter is already non–baryonic.

3. Star Formation Law

Following the pioneering work of Schmidt (1959), it is common to relate gas density to the SFR density using a power law. Although originally formulated in terms of volume densities, for a constant scale height disk the Schmidt–law can be written as $\Sigma_{SFR} \sim (\Sigma_{gas})^N$. The value of N has been found in the literature to cover a range of 0.9 to 3.5 (see Bigiel *et al.* 2008, for a summary). Kennicutt (1998), extending his earlier work (Kennicutt 1989), studied the relation between the disk–averaged SFR surface density and gas surface density, finding $N = 1.4 \pm 0.15$. Using THINGS we are now able to investigate the relation between SFR surface density and gas surface density on a pixel by pixel basis, the pixels being chosen to be at a common linear resolution of 750 pc. We use a linear combination of *GALEX* FUV and *Spitzer* 24 μm emission to determine the SFR. A full account of how this is done is given in the appendix of Leroy *et al.* (2008a). Moreover, we can investigate the Schmidt–Kennicutt law for just the neutral atomic gas (H I), for the molecular gas (H_2 as traced by CO), and for the total gas surface density (H I+H_2).

This is illustrated in Fig. 3 where we plot $\log \Sigma_{\rm SFR}$ (the log of the SFR surface density) against $\log \Sigma_{\rm H\,I}$, $\log \Sigma_{\rm H_2}$, and $\log \Sigma_{\rm H\,I+H_2}$ (see figure caption for details). In the paper by Bigiel *et al.* (2008) we find that the $\Sigma_{\rm SFR}$ and $\Sigma_{\rm H_2}$ obey a tight Schmidt–type power law with index $N = 1.0 \pm 0.2$, i.e., H_2 forms stars at a constant efficiency in the disks of spiral galaxies. The average molecular gas depletion time is $\sim 2 \times 10^9$ years. We interpret the linear relation and constant depletion time as evidence that stars in the disks of spirals are forming in GMCs with approximately uniform properties and that $\Sigma_{\rm H_2}$ may be a measure of the filling fraction of GMCs rather than real variations in surface density. The relationship between total gas surface density $\Sigma_{\rm H\,I+H_2}$ and $\Sigma_{\rm SFR}$ varies dramatically among and within spiral galaxies which is due to the fact that most galaxies show little or no correlation between $\Sigma_{\rm H\,I}$ and $\Sigma_{\rm SFR}$. In addition to a molecular Schmidt law, the other general feature of our sample is a sharp saturation of H I surface densities at $\Sigma_{\rm H\,I} = 9\,{\rm M_\odot\,pc^{-2}}$ (or $12\,{\rm M_\odot\,pc^{-2}}$ when including He) above which we observe gas to be molecular.

4. H I Supershells

The superior resolution and sensitivity of THINGS reveals a wealth of structure in the ISM of gas–rich systems and is exploited in a paper by Bagetakos *et al.* (2008). Fig. 4, adapted from their paper, shows as example the H I surface brightness map of NGC 6946. The H I closely traces the flocculent spiral arms. In addition, a large number of elliptical features can be seen, both in the H I surface brightness maps as well as in the data cubes. They have in the past been described as H I shells or supershells (depending

https://doi.org/10.1017/S1743921308027725 Published online by Cambridge University Press

on their size), H I superbubbles, or H I holes. For the remainder of this paper we refer to them as H I holes as this is how they appear in maps and avoids prejudicing their interpretation.

The most widely accepted explanation for the origin of H I holes is that they are due to the almost instantaneous deposition of kinetic energy as the result of Type II supernovae from rapidly evolving, massive stars which formed in super star clusters (SSCs) or OB associations (Oey & Clarke 1997). We have detected more than 1000 holes in a total of 20 galaxies. This is the first time that the same detection technique is applied using such a large data set of uniformly high quality. The sizes of the H I holes range from about 100 pc (our resolution limit) to 2000 pc. Their expansion velocities vary from 5 to 35 $\mathrm{km\,s^{-1}}$. We estimate their ages at 6 – 150 Myr and their energy requirements, based on a simple single blast approximation (Chevalier 1974), at $10^{50} - 10^{53}$ erg. In most galaxies, H I holes are found all the way out to the edge of the H I disk. Assuming that holes are the result of massive star formation we estimate the star formation rate and find that it correlates with values obtained by other SF tracers, lending support to the idea that H I holes and SF are linked. We also calculated the 2– and 3–dimensional porosity of the ISM in the galaxies studied and find that it tends to increase from early–type spirals to dwarf

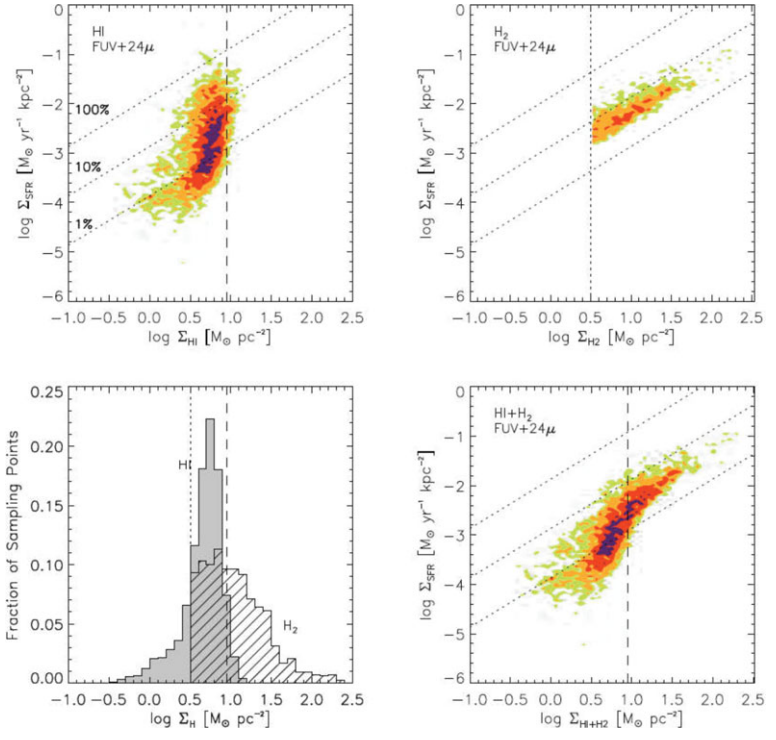

Figure 3. Plots of $\log \Sigma_{\mathrm{SFR}}$ versus $\log \Sigma_{\mathrm{H\,I}}$ (top left), $\log \Sigma_{\mathrm{H_2}}$ (top right), and $\log \Sigma_{\mathrm{H\,I+H_2}}$ (bottom right); the results for 7 spiral galaxies are plotted together in these diagrams. Diagonal dotted lines show lines of constant SFE, indicating the level of SFR needed to consume 1%, 10% and 100% of the gas reservoir (including helium) in 10^8 years. Thus, the lines also correspond to constant gas depletion times of, from top to bottom, 10^8, 10^9, and 10^{10} yr. The bottom left panel shows the normalized distribution of H I and H_2 surface densities in the sample. The dashed vertical line is drawn at $9\,\mathrm{M_\odot\,pc^{-2}}$ which is where we observe gas in excess of this surface density to be in the molecular phase; the dotted vertical line corresponds to the sensitivity of the CO observations used to infer the H_2 column density and lies at $3\,\mathrm{M_\odot\,pc^{-2}}$ (figure taken and adapted from Bigiel *et al.* 2008).

https://doi.org/10.1017/S1743921308027725 Published online by Cambridge University Press

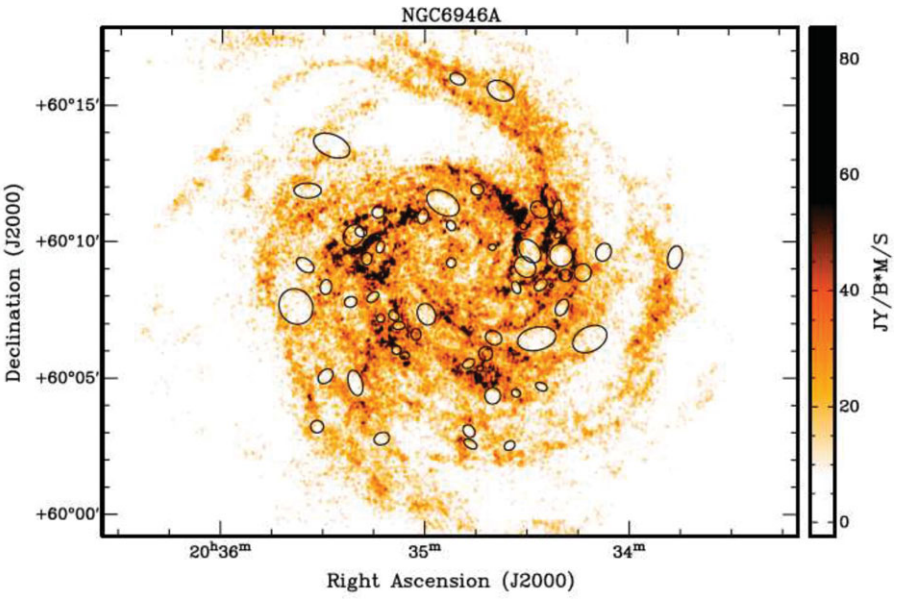

Figure 4. Location of H I holes in NGC 6946. The size and orientation of the ellipses indicate the location and approximate orientation and observed size of the H I holes.

galaxies, as predicted by Silk (1997) which is suggestive of the fact that self–regulation plays an important rôle in setting the SFR in galaxies.

References

Bigiel, F., Leroy, A., Walter, F., Brinks, E., de Blok, W. J. G., Madore, B., & Thornley, M. D. 2008, *AJ* (submitted)

Bagetakos, I., Brinks, E., Walter, F., de Blok, W. J. G., Rich, J. W., Usero, A., & Kennicutt, R. C., Jr. 2008, *AJ* (submitted)

Chevalier, R. A. 1974, *ApJ*, 188, 501

de Blok, W. J. G., Walter, F., Brinks, E., Trachternach, C., Oh, S.-H., & Kennicutt, R. C., Jr. 2008, *AJ* (accepted)

Gil de Paz, A., *et al.* 2007, *ApJS*, 173, 185

Kennicutt, R. C. 1989, *ApJ*, 344, 685

Kennicutt, R. C. 1998, *ApJ*, 498, 541

Kennicutt, R. C., Jr., *et al.* 2003, *PASP*, 115, 928

Leroy, A., Walter, F., Brinks, E., Bigiel, F., de Blok, W. J. G., Madore, B., & Thornley, M. D. 2008a, *AJ* (submitted)

Leroy, A., Walter, F., Bigiel, F., Weiß, A., Usero, A., Brinks, E., de Blok, W. J. G., & Kennicutt, R. C., Jr. 2008b, *AJ* (submitted)

Oh, S.-H., de Blok, W. J. G., Walter, F., Brinks, E., & Kennicutt, R. C., Jr. 2008, *AJ* (accepted)

Oey, M. S. & Clarke, C. J. 1997, *MNRAS*, 289, 570

Schmidt, M. 1959, *ApJ*, 129, 243

Silk, J. 1997, *ApJ*, 481, 703

Trachternach, C., de Blok, W. J. G., Walter, F., Brinks, E., & Kennicutt, R. C., Jr. 2008, *AJ* (submitted)

Usero, A., Brinks, E., Walter, F., de Blok, W. J. G., & Kennicutt, R. C., Jr. 2008, *AJ* (submitted)

Walter, F., Brinks, E., de Blok, W. J. G., Bigiel, F., Kennicutt, R. C., Jr., Thornley, M. D., & Leroy, A. 2008, *AJ* (accepted)

https://doi.org/10.1017/S1743921308027725 Published online by Cambridge University Press